



<b>Title</b>	Molecular dynamics study of water in contact with TiO <sub>2</sub> rutile-110, 100, 101, 001 and anatase-101, 001 surface
<b>Authors(s)</b>	Kavathekar, Ritwik S., Dev, Pratibha, English, Niall J., MacElroy, J. M. Don
<b>Publication date</b>	2011-05-19
<b>Publication information</b>	Kavathekar, Ritwik S., Pratibha Dev, Niall J. English, and J. M. Don MacElroy. "Molecular Dynamics Study of Water in Contact with TiO <sub>2</sub> Rutile-110, 100, 101, 001 and Anatase-101, 001 Surface" 109, no. 13 (May 19, 2011).
<b>Publisher</b>	Taylor and Francis
<b>Item record/more information</b>	<a href="http://hdl.handle.net/10197/2961">http://hdl.handle.net/10197/2961</a>
<b>Publisher's statement</b>	This is an electronic version of an article published in Kavathekar, Ritwik S. , Dev, Pratibha , English, Niall J. and MacElroy, J. M. D.(2011) 'Molecular dynamics study of water in contact with the TiO <sub>2</sub> rutile-110, 100, 101, 001 and anatase-101, 001 surface', Molecular Physics,, First published on: 19 May 2011 (iFirst), available online at <a href="http://dx.doi.org/10.1080/00268976.2011.582051">http://dx.doi.org/10.1080/00268976.2011.582051</a>
<b>Publisher's version (DOI)</b>	10.1080/00268976.2011.582051

Downloaded 2023-10-05T14:16:07Z

The UCD community has made this article openly available. Please share how this access benefits you. Your story matters! (@ucd\_oa)



© Some rights reserved. For more information

## RESEARCH ARTICLE

### **Molecular dynamics study of water in contact with TiO<sub>2</sub> rutile-110, 100, 101, 001 and anatase-101, 001 surface**

Ritwik S. Kavathekar <sup>a</sup>, Pratibha Dev <sup>a</sup>, Niall J. English <sup>a\*</sup> and J.M.D. MacElroy <sup>a</sup>

<sup>a</sup> *The SFI Strategic Research Cluster in Solar Energy Conversion and the Centre for Synthesis and Chemical Biology, School of Chemical and Bioprocess Engineering, University College Dublin, Belfield, Dublin 4, Ireland.*

\* Corresponding author:

Dr Niall English,  
School of Chemical and Bioprocess Engineering,  
University College Dublin,  
Belfield, Dublin 4, Ireland.  
niall.english@ucd.ie  
Phone: +353(1)716 1646

# Molecular dynamics study of water in contact with TiO<sub>2</sub> rutile-110, 100, 101, 001 and anatase-101, 001 surface

We have carried out classical molecular dynamics of various surfaces of TiO<sub>2</sub> with its interface with water. We report the geometrical features of the first and second monolayers of water using a Matsui Akaogi (MA) force field for the TiO<sub>2</sub> surface and a flexible single point charge model for the water molecules. We show that the MA force field can be applied to surfaces other than Rutile-(110). It was found that water OH bond lengths, H-O-H bond angles and dipole moments do not vary due to the nature of the surface. However, their orientation within the first and second monolayers suggest that planar Rutile-(001) and Anatase-(001) surfaces may play an important role in not hindering removal of the products formed on these surfaces. Also, we discuss the effect of surface termination in order to explain the layering of water molecules throughout the simulation box.

Keywords: molecular dynamics, TiO<sub>2</sub> surface, oxide-water interface, rutile, anatase

## 1. Introduction

Titanium dioxide (TiO<sub>2</sub>) surfaces have been of most interest for photochemical degradation of organic compounds as bactericides, hydrophobic coatings, [1] and show considerable potential in the field of solar energy conversion by mediation of photocatalytic splitting of water, as demonstrated by the Fujishma-Honda reaction [2]. This reaction is a four-hole mechanism, [3] producing O<sub>2</sub>/H<sub>2</sub> gas, and takes place in the presence of solar radiation and in the absence of external bias. Electron-hole pairs are generated in the bulk and migrate towards the surface where the hole reacts with water. Although several materials have been used as photocatalysts for H<sub>2</sub>/O<sub>2</sub> production, like nanoribbons of CdSe-MoS<sub>2</sub>, [4] core (GaN:ZnO)-shell (Cr<sub>2</sub>O<sub>3</sub>),[5] oxynitrides,[6] BiVO on reduced graphene,[7] phosphate-based Co<sup>2+</sup> catalysts,[8] algae,[9] and, more recently, Fe<sub>2</sub>O<sub>3</sub>,[10] TiO<sub>2</sub> remains a strong contender due to its stability, cost-effectiveness and non-toxicity. It is clear that the structure of TiO<sub>2</sub>-water interface plays a great role in enhancing efficiency of photolysis. Rutile is the most abundant polymorph of TiO<sub>2</sub> and the (110) face is the most stable surface. The pristine (110) surface is inert but water splitting takes place at defect sites [11] created by oxygen vacancies, and much experimental [12] and theoretical [13-

16] scrutiny has been directed consequently thereto. Water molecules may undergo dissociative or molecular adsorption or both [1]. One of the early calculations [17] proposing mixed water absorption based on first principles was done by Lindan *et.al.* Quasielastic neutron scattering (QENS) studies along with molecular dynamics (MD) [18] have demonstrated that water molecules form hydrogen-bonded second and third layers above the (110) surface. Back-scattering neutron spectroscopy reports, [19] supported by MD, show that, on average, participation of water molecules in four hydrogen bonds is needed for slow dynamical (“Arrhenius type”) behaviour, while that dynamics (“non-Arrhenius type”) is possible if less than three hydrogen bonds are present, depending on the level of hydration. Most of the reported work [15,16,20] on water adsorption on rutile-(110) deals with adsorption isotherm prediction, surface charging effects using the multisite complexation model (MUSIC) and correlating behaviour with pH titration employing both classical and quantum chemical approaches. Density functional theory using plane-augmented wave potentials have been used [15] to model photooxidation of water with detailed energetic analysis. Also some solvation studies of TiO<sub>2</sub> surfaces using reaction fields and conductor-like, screening models for real solvents (COSMO-RS) have been reported [16] for predicting proton affinity to the surface. Another important rutile surface is (100), which, along with (110), contributes to the reaction mechanism of photocatalytic water-splitting. *Ab initio* simulations based on Car-Parrinello Molecular Dynamics (CPMD) on perfect and defect rutile-(110) and rutile-(100) surfaces [21] resulted only in weakly stabilized H<sub>2</sub>O molecule on the pristine surface. But OH dissociation was observed on defects (creation of an oxygen vacancy) rutile-(100) surface and not on the perfect or defect rutile-(110) as postulated. Rutile (101) contributes to about 20% of the bulk surface, along with rutile-(100), and thus these constitute particularly important surfaces for water absorption. Although most

studies have been performed using quantum methods, classical dynamics remains an important tool for studying larger picosecond time scale phenomenon with macroscopically observed properties.

## 2. Simulation Methodology

Anhydrous rutile-(110), (100), (101), (001) and anatase-(101), (001) surface geometries were realised in slab configurations in the  $x$ - $y$  plane and water molecules added in the  $z$ -direction for at least 50 Å distance. The respective molecular compositions and structural details for relaxed water-titania interfaces are specified in Table I. [Insert Table 1 near here] Classical molecular dynamics was performed in the NVT ensemble at 300 K using DL\_POLY [22] in conjunction with a Nosé-Hoover thermostat, the 3D Ewald summation for long-range electrostatic interactions with an accuracy of  $10^{-5}$  and the Velocity-Verlet scheme with a time step of 1 fs. All production simulations were run for 1 ns after 200 ps of equilibration. All simulations were periodic in three dimensions. We used the force field as reported by Bandura *et.al.* [14] and Predota *et.al.* [20] for all surfaces and the water model and cross interaction parameters are summarised in Table II. [Insert Table near here] For the crystal, the Matsui and Akaogi (MA) [23] parameters were used, while water was represented by a Lennard-Jones potential with a harmonic  $H_w-O_w-H_w$  angle potential and a Morse-stretch  $O_w-H_w$  bond potential. Water bond angles and bond lengths were not constrained and thus a flexible SPC model was used. Using a classical morse stretching potential enables one to follow bond length changes during the course of the simulation. This is however a non-dissociative model and is thus unable to reproduce water splitting or OH dissociation. In the present work, we are only interested in the orientation and detection of any strain on the water molecules within the monolayers. The entire  $TiO_2$  block was mobile for all surfaces throughout the simulation.

Bulk rutile is defined by lattice vectors of length  $a_0=b_0= 4.593 \text{ \AA}$ ,  $c_0=2.959 \text{ \AA}$  with symmetry group  $P42/MNM$ . Bulk anatase has lattice vectors  $a_0=b_0= 3.776 \text{ \AA}$  and  $c_0=9.486 \text{ \AA}$  and a symmetry group  $I41/AMD$ . All surfaces were constructed by cleaving super cells made from bulk crystals. The rutile-(110) surface (Fig. 1A) is the most thermodynamically stable and constitutes a major part of the bulk  $\text{TiO}_2$  surface. [Insert Figure 1 near here] The (110) surface was reconstructed for charge auto-compensation [1]. The rutile (110) oxygen-terminated surface is non-polar [24] and hence a dipole-free surface was ensured. The rutile (110) surface consists of bridging oxygen atoms bonded to 6-coordinated titania ( $\text{Ti}_{6c}$ ) and a 3-coordinated oxygen ( $\text{O}_{3c}$ ) bonded to  $\text{Ti}_{5c}$  and  $\text{Ti}_{6c}$  atoms. These  $\text{Ti}_{5c}$  surface atoms were used as the plane against which height measurements of water oxygen ( $\text{O}_w$ ) atoms were made. Surface termination produces coordinatively unsaturated –sites (CUS), which differ in charge from the bulk. Although surface-modified charges are available [14] for the rutile (110) surface, they have not been specified for other surfaces, to the best of the authors' knowledge. The rutile (100) surface (Fig. 1(B)) constitutes about 20% of the bulk rutile and has a ridge pattern created by 2-coordinated bridging oxygen atoms connected to  $\text{Ti}_{5c}$ . The rutile (100) surface is similar to that of rutile (110), except that the bridging plane of  $\text{Ti}_{5c}\text{--O}_b\text{--Ti}_{5c}$  is inclined at an angle, rather than perpendicular as in (110). The rutile (101) plane (Fig 1(C)) is similar to that of rutile (100) and also composes 20% of naturally occurring rutile. It is also composed of  $\text{Ti}_{5c}$  and  $\text{O}_{2c}$  structures, but the  $\text{Ti}_{5c}$  bond length differs to the  $\text{O}_{2c}$  creating two different types of  $\text{O}_{2c}$ . Also, the rutile (101) plane is tilted with respect to the  $z$ -direction (chosen as the standard orientation for solvation, as mentioned previously), and was rotated for alignment vis-à-vis the  $z$ -direction. The rutile-(001) surface (Fig. 1(D)) forms a lesser part of naturally occurring rutile, and although only a few experiments have been performed on this surface, it was considered in this study for the sake of completeness and

comparison. The rutile-(001) surface has 4-coordinated Ti atoms ( $Ti_{4c}$ ) bonded to  $O_{2c}$  atoms, along with alternating  $Ti_{6c}$  atoms bonded to  $O_{2c}$  atoms, giving it a corrugated, ridge-like structure. This surface is comparatively more acidic due to large-coordinate unsaturation (CUS) of  $Ti_{4c}$  atoms. It is also unstable and hence difficult to experimentally study due to spontaneous reconstruction of the surface.

Anatase is the more photoactive polymorph and is also proposed [25] to be an efficient candidate for photoelectrolysis of water. It is also used in other solar energy-based applications like dye sensitized solar cells, and therefore the water-anatase interface constitutes an important system for comparative studies vis-à-vis rutile. The anatase (101) surface (Fig 2(A)) exhibits a terrace-like structure formed by fully-coordinated  $Ti_{6c}$  atoms bonded to  $O_{3c}$  atoms and under-coordinated  $Ti_{5c}$  with  $O_{2c}$ . [Insert Figure 2 near here] The surface is tilted at an angle with respect to the [101] direction and was rotated to align with the  $z$ -axis, *i.e.*, [001]. Although the pristine anatase (101) surface is inert to photolysis, some reports have indicated dissociative adsorption onto anatase-(001) surfaces [25]. The anatase-(001) face is not stable, and various instances of this have been reported [1]. Anatase-(001) (Fig 2(B)) has a flat plane connected by alternating rows of  $Ti_{5c}$  and  $O_{2c}$  atoms in a three- and two-fold manner, respectively. Surfaces can be made non-polar [24] by varying the surface termination. This surface dipole effect was manifested in our simulations wherein water was found to layer on top of such dipole “not-free” surfaces.

### 3. Results and Discussion

The density distributions, based on the distance of the water oxygen ( $O_w$ ) atoms from the crystal plane, are depicted in Fig. 3. [insert Figure 3 near here] The density of water was calculated as the mass of number of water molecules per  $0.1 \text{ \AA}$  volume increment away from the surface

(counting a molecule present if its  $O_w$  is in each grid-element), *i.e.*, along the direction of heterogeneity (the  $z$ -direction). This density profile was used as a guide to sample respective properties in consecutive layers. Fig. 3a shows the order of distance to the rutile plane is  $(100) < (101) < (110) = (001)$ . The plane used for calculation of the distance to  $O_w$  atoms was taken to be the first Ti plane found on the surface. The distance for rutile-(100) is found to be 1.9 Å, due to the (electrostatic) attraction of  $Ti_{5c}$  atoms below the  $O_{2c}$  to the water oxygen atoms. This is similar to the (101)-case, for which the first exposed plane is formed by  $O_{2c}$  atoms, but the  $Ti_{5c}$  atoms are bonded to the  $O_{2c}$  atoms in the same plane, and hence the water oxygen atoms are at approximately 2.3 Å distance due to  $O_{2c}$ - $O_w$  repulsion compensated by  $Ti_{5c}$ - $O_{2c}$  attraction. The (110)-surface plane was taken to be that formed by  $Ti_{5c}$  rather than the bridging oxygen atoms. Water molecules occupy the spaces in between the  $Ti_{5c}$  (probably owing to the tetrahedral water geometry formed by two hydrogen atoms and two lone pairs), rather than on top of it. For the (001) surface, alternated with  $O_{2c}$  and  $Ti_{4c}$  sites, the  $H_w$  are therefore tilted towards the  $O_{2c}$  atoms, creating a tilt angle and 'pulling' the water molecule inwards. For anatase surfaces, the order of distance to the plane is in the order  $(101) < (001)$ . The (101) ridged, terrace-like structure permits the water molecules to remain in-between the  $O_{2c}$  atoms, binding more weakly to the  $Ti_{5c}$  surface atoms, whilst remaining hydrogen-bonded to  $O_{2c}$  atoms. The anatase-(001), planar surface creates a flat monolayer, at a distance of 2.5 Å. Previous calculations using similar force fields have been reported [20] and references therein. However these simulations [20] were performed on stationary surfaces derived from quantum simulations with a rigid SPC water model, 3D Ewald sum with correction for 2D periodic geometry electrostatics at 298.15 K temperature. They reported a  $z$  axis density profile distance for water oxygens at 2.2 Å for neutral rutile-(110) surface. CPMD simulations [26] for anatase-(101) and (001) surfaces showed



dissociative adsorption of water molecules on anatase-(001). The  $Ti_{5c}-O_w$  (dissociated water) distance was reported 1.84 Å and  $Ti_{5c}-O_w$  (molecular water) observed at 2.14. They observed no dissociation on pristine anatase-(101). [Insert Figure 4 and 5 near here]

In order to investigate intramolecular strain in the water molecules at the interface we calculated as depicted Figs. 4 and 5 respectively the probability distributions of water ( $H_w-O_w-H_w$ ) angles and  $O_w-H_w$  bond lengths in the adsorbed monolayer (evident from the density profiles of Fig. 3, and labeled as 'L1'). However no significant shifts were found for interfacial, adsorbed water molecules relative to bulk water molecules. The average bond angle in the adsorbed layer was  $106.11^\circ$  compared to  $107.22^\circ$  in the bulk for the rutile-(101) case, while for the anatase-(101) case, the adsorbed layer's angle was  $105.55^\circ$  compared to  $106.66^\circ$  in the bulk liquid. Also the  $O_w-H_w$  bond length showed no significant deviation L1 and bulk, with the average bond length (Fig. 5) being 1.02 Å. This geometry is close to the values of  $108.5^\circ$  and 0.98 Å for the water angle and bond length respectively, reported [27] by plane wave based *ab initio* DFT using GGA functional on rutile-(110) surface, which were modeled for STM experiments. [Insert Figure 7 near here]

We calculated distribution profiles for molecular dipole moment of water (Fig. 6) in L1 and found its average value to be at 2.4 D, without significant deviation from the other layers and is consistent with the value of condensed water [28] at all interfaces. This is consistent with water bond angles and bond lengths in all the simulations. [Insert Figure 7 near here] Figure 7 shows angle made by a vector on the titania surface and the molecular dipole moment vector of water. It is seen that at the rutile-(110)-water interface, dipole vector points downwards making a  $90^\circ$  angle with the surface. However, for rutile-(001) and anatase-(001) surfaces, the vectors are pointed along the surface on either side. Water dipole vectors at the rutile-(100) surface are

oriented in one direction along the surface while, for rutile-(101) water dipole vectors are pointing towards and along the surface. Sampling between the regions within 5 Å of the interface involves at least two water monolayers, as seen in Figs. 3. Calculating water dipole moment vectors at these monolayer distances resolves the orientation more clearly, as shown in Fig 8. Rutile-(110) (Fig. 8(A)) distinguishes between the first and second monolayer (ML) dipole vector orientations of water at distance of 2.4 Å and 3.9 Å respectively. [Insert Figure 8 near here] The first ML water molecules are oriented perpendicular to the surface as depicted in Fig 1A (black/dark shade) and the second ML (yellow/light shade) dipole moment vectors to be pointing along either sides of the surface. Water molecules in both the monolayers are stabilized by hydrogen bonding with bridging oxygens' of rutile-(110). Rutile-(100) face has a slanting roof-like structure with bridging oxygens' at the edges: hence their angles are off to one side along the surface (Fig 1(B)), with first ML and second ML waters appearing at distances of 1.9 Å and 3.1 Å respectively. The first ML and second ML for rutile-(101) appear at 2.3 Å and 3.6 Å with a spread of angles in the second ML and a partial orientation in the first ML, owing to the serrated nature of the surface. The second ML waters have H<sub>w</sub> atoms bonding with bridging oxygens' with O<sub>w</sub> pointing opposite to the *z*-direction and the first ML waters are spread in a perpendicular direction with O<sub>w</sub> pointing towards Ti<sub>5c</sub>. The rutile-(001) surface is planar, wherein Ti<sub>4c</sub> atoms are sandwiched between O<sub>2c</sub> competing with H-bonding with water molecules, giving them an angular orientation with O<sub>w</sub> pointing towards Ti<sub>4c</sub>. This pushes the second ML away to 5.2 Å from the first ML at 2.4 Å. A small shoulder at 2.8 Å in the density distribution of rutile-(001) (Fig. 3(A)) indicates a second orientation within the first ML with H<sub>w</sub> pointing towards O<sub>2c</sub> atoms. The anatase-(101) surface is similar to rutile-(100) except that Ti and O layers alternate in the *x*-direction hence their angles are similar, *i.e.*, along the surfaces.

The anatase-(101) first ML and second ML occur at 2.4 Å and 3.8 Å respectively. Anatase-(001), like the rutile-(001) is a planar surface but much flatter without any “cavities”, thus creating a denser and uniform first and second monolayers. The anatase-(001) first and second ML are at 2.9 Å and 5.7 Å respectively.

#### 4. Conclusions

We have performed classical molecular dynamics of rutile (110), (101), (001), (001) and anatase (101), (001) faces for polymorphs of TiO<sub>2</sub> in contact with water, using a flexible Morse potential for water and Matsui-Akaogi potential for the crystal, wherein the entire crystal block is mobile and not fixed/constrained. Newer force field models employing polarization effects, as recently suggested by Han *et.al.* [29] would be a good approach to model the flexible lattice. This is due to the fact that phonon dispersion curves have been fitted with *ab initio* density functional theory (LDA) to the classical force field model. The orientation of water molecules depends heavily on the surface terminations of either side of the solid surfaces. Analysis of the distribution profiles of O<sub>w</sub>H<sub>w</sub> bond lengths and H<sub>w</sub>-O<sub>w</sub>-H<sub>w</sub> angles show no considerable shift from their equilibrium values along the sampled layers. The orientation of water molecules in the first and second monolayer is considerably influenced by the nature of the surface. The mobile crystal surface influences the water monolayer dynamics wherein orientation and bonding properties fluctuate rapidly. At a temperature of 300K, this leads to a weakly bound first monolayer as compared to the static/fixed lattice. The geometry of water molecules is similar to that reported by quantum simulations [27]. For planar surfaces the second monolayer is further pushed thereby affecting any stabilizing role played by secondary solvation of the charge transfer products/adducts created at the first ML after photoexcitation of the crystal. It can be said that rutile-(001) and anatase-(001) surfaces may play an important role by not hindering the removal of products (H<sub>2</sub>/O<sub>2</sub>)

formed at the first monolayer, which is a major problem with other surfaces [30]. It has been shown that these interactions between the first and second monolayer through hydrogen bonding depending on the rigidity of the first monolayer. Hopefully these simulations will provide insights into modelling large scale simulations or macroscopic single crystal or an ensemble of such particles in contact with water [31].

### **Acknowledgements**

The authors acknowledge useful conversations with Dr. Damian Mooney. This material is based upon works supported by the Science Foundation Ireland (SFI) under grant No. 07/SRC/B1160, in addition to the Irish Research Council for Science, Engineering and Technology. We also thank SFI and the Irish Centre for High End Computing for the provision of high-performance computing facilities.

## References

- [1] U. Diebold, *Surface Science Reports* **48** (5-8), 53 (2003)
- [2] A. Fujishima and K. Honda, *Nature* **238** (5358), 37 (1972)
- [3] J. W. Tang, J. R. Durrant, and D. R. Klug, *J. Am. Chem. Soc.* **130** (42), 13885 (2008)
- [4] F. A. Frame and F. E. Osterloh, *J. Phys. Chem. C* **114** (23), 10628 (2010)
- [5] K. Maeda, N. Sakamoto, T. Ikeda, H. Ohtsuka, A. K. Xiong, D. L. Lu, M. Kanehara, T. Teranishi, and K. Domen, *Chem.-Eur. J.* **16** (26), 7750 (2010)
- [6] K. Maeda, M. Higashi, D. L. Lu, R. Abe, and K. Domen, *J. Am. Chem. Soc.* **132** (16), 5858 (2010)
- [7] Y. H. Ng, A. Iwase, A. Kudo, and R. Amal, *J. Phys. Chem. Lett.* **1** (17), 2607 (2010)
- [8] M. W. Kanan and D. G. Nocera, *Science* **321** (5892), 1072 (2008)
- [9] A. Melis and T. Happe, *Plant Physiology* **127** (3), 740 (2001)
- [10] Kevin Sivula, Radek Zboril, Florian Le Formal, Rosa Robert, Anke Weidenkaff, Jiri Tucek, Jiri Frydrych, and Michael Gratzel, *J. Am. Chem. Soc.* **132** (21), 7436 (2010)
- [11] O. Bikondoa, C. L. Pang, R. Ithnin, C. A. Muryn, H. Onishi, and G. Thornton, *Nature Materials* **5** (3), 189 (2006)
- [12] E. Wahlstrom, E. K. Vestergaard, R. Schaub, A. Ronnau, M. Vestergaard, E. Laegsgaard, I. Stensgaard, and F. Besenbacher, *Science* **303** (5657), 511 (2004); K. Onda, B. Li, J. Zhao, K. D. Jordan, J. L. Yang, and H. Petek, *Science* **308** (5725), 1154 (2005); R. Nakamura, T. Okamura, N. Ohashi, A. Imanishi, and Y. Nakato, *J. Am. Chem. Soc.* **127** (37), 12975 (2005); F. Allegretti, S. O'Brien, M. Polcik, D. I. Sayago, and D. P. Woodruff, *Phys. Rev. Lett.* **95** (22), 4 (2005); I. M. Brookes, C. A. Muryn, and G. Thornton, *Phys. Rev. Lett.* **87** (26), 4 (2001)
- [13] Scott J. Thompson and Steven P. Lewis, *Physical Review B* **73** (7), 073403 (2006); M. L. Machesky, M. Predota, D. J. Wesolowski, L. Vlcek, P. T. Cummings, J. Rosenqvist, M. K. Ridley, J. D. Kubicki, A. V. Bandura, N. Kumar, and J. O. Sofo, *Langmuir* **24** (21), 12331 (2008); M. Machesky, M. Ridley, D. Wesolowski, D. Palmer, M. Predota, L. Vlcek, J. Kubicki, J. Sofo, A. Bandura, Z. Zhang, and P. Fenter, *Geochimica Et Cosmochimica Acta* **71** (15), A609 (2007); L. Vlcek, Z. Zhang, M. L. Machesky, P. Fenter, J. Rosenqvist, D. J. Wesolowski, L. M. Anovitz, M. Predota, and P. T. Cummings, *Langmuir* **23** (9), 4925 (2007); N. Kumar, S. Neogi, P. R. C. Kent, A. V. Bandura, J. D. Kubicki, D. J. Wesolowski, D. Cole, and J. O. Sofo, *J. Phys. Chem. C* **113** (31), 13732 (2009)
- [14] A. V. Bandura and J. D. Kubicki, *J. Phys. Chem. B* **107** (40), 11072 (2003)
- [15] A. Valdes, Z. W. Qu, G. J. Kroes, J. Rossmeisl, and J. K. Nørskov, *J. Phys. Chem. C* **112** (26), 9872 (2008)
- [16] P. Zarzycki, *J. Phys. Chem. C* **111** (21), 7692 (2007)
- [17] Philip J. D. Lindan, N. M. Harrison, and M. J. Gillan, *Phys. Rev. Lett.* **80** (4), 762 (1998)
- [18] E. Mamontov, L. Vlcek, D. J. Wesolowski, P. T. Cummings, W. Wang, L. M. Anovitz, J. Rosenqvist, C. M. Brown, and V. G. Sakai, *J. Phys. Chem. C* **111** (11), 4328 (2007)
- [19] E. Mamontov, D. J. Wesolowski, L. Vlcek, P. T. Cummings, J. Rosenqvist, W. Wang, and D. R. Cole, *J. Phys. Chem. C* **112** (32), 12334 (2008)
- [20] M. Predota, A. V. Bandura, P. T. Cummings, J. D. Kubicki, D. J. Wesolowski, A. A. Chialvo, and M. L. Machesky, *J. Phys. Chem. B* **108** (32), 12049 (2004)
- [21] W. Langel, *Surface Science* **496** (1-2), 141 (2002)

- [22] M. Leslie W. Smith, T.R. Forester, *The DL\_POLY\_2 User Manual*, edited by Editor v. 2.14 ed. (2003).
- [23] M. Matsui and M. Akaogi, *Mol. Sim.* **6**, 239 (1991)
- [24] Jacek. Goniakowski, Fabio. Finocchi, and Claudine. Noguera, *Reports on Progress in Physics* **71** (1), 016501 (2008)
- [25] Annabella Selloni, *Nature Materials* **7** (8), 613 (2008)
- [26] M. Sumita, C. P. Hu, and Y. Tateyama, *J. Phys. Chem. C* **114** (43), 18529 (2010)
- [27] G. Teobaldi, W. A. Hofer, O. Bikondoa, C. L. Pang, G. Cabailh, and G. Thornton, *Chemical Physics Letters* **437** (1-3), 73 (2007)
- [28] J. K. Gregory, D. C. Clary, K. Liu, M. G. Brown, and R. J. Saykally, *Science* **275** (5301), 814 (1997)
- [29] X. J. Han, L. Bergqvist, P. H. Dederichs, uuml, H. Iler-Krumbhaar, J. K. Christie, S. Scandolo, and P. Tangney, *Physical Review B* **81**, 134108 (2010)
- [30] L. M. Liu, P. Crawford, and P. Hu, *Progress in Surface Science* **84** (5-6), 155 (2009); D. Pillay, Y. Wang, and G. S. Hwang, *J. Am. Chem. Soc.* **128** (43), 14000 (2006)
- [31] A. S. Barnard, P. Zapol, and L. A. Curtiss, *Journal of Chemical Theory and Computation* **1** (1), 107 (2005)

## Figure Captions

- Fig. 1: Representative configurations of various rutile-water interfaces: (A) (110), (B) (100), (C) (101), and (D) (001).
- Fig. 2: Representative configurations of various anatase-water interfaces: (A) (101), and (B) (001)
- Fig. 3: Absolute density ( $\text{gm cm}^{-3}$ ) of water above various planes of (a) rutile and (b) anatase. The plane formed by the first surface titanium atoms was used for projection of the vectors (see text for details).
- Fig. 4: Probability distribution of the water  $\text{H}_w\text{-O}_w\text{-H}_w$  angle in the adsorbed monolayer in contact with each surface.
- Fig. 5: Distribution of the water  $\text{O}_w\text{-H}_w$  bond length in the adsorbed monolayer in contact with each surface.
- Fig. 6: Distribution of the water absolute dipole moment in the adsorbed monolayer in contact with each surface.
- Fig. 7: Distribution of the cosine of angle of the monolayer's water molecules' dipole vectors with respect to the plane of the crystal surfaces,  $\theta$ , for various faces of (a) rutile, and (b) anatase. A cosine of zero indicates dipole alignment normal to the face, while  $\pm 1$  indicates parallel dipole alignment, oriented parallel, or along, the surface.
- Fig. 8: Distribution of the cosine of angle of the first two layers of water molecules' dipole vectors with respect to the plane of the crystal surfaces,  $\theta$ , for various faces: (A) Rutile (110), (B) Rutile (100), (C) Rutile (101), (D) Rutile (001), (E) Anatase (101), (F) Anatase (001). A cosine of zero indicates dipole alignment normal to the face, while  $\pm 1$  indicates parallel dipole alignment, oriented parallel, or along, the surface.

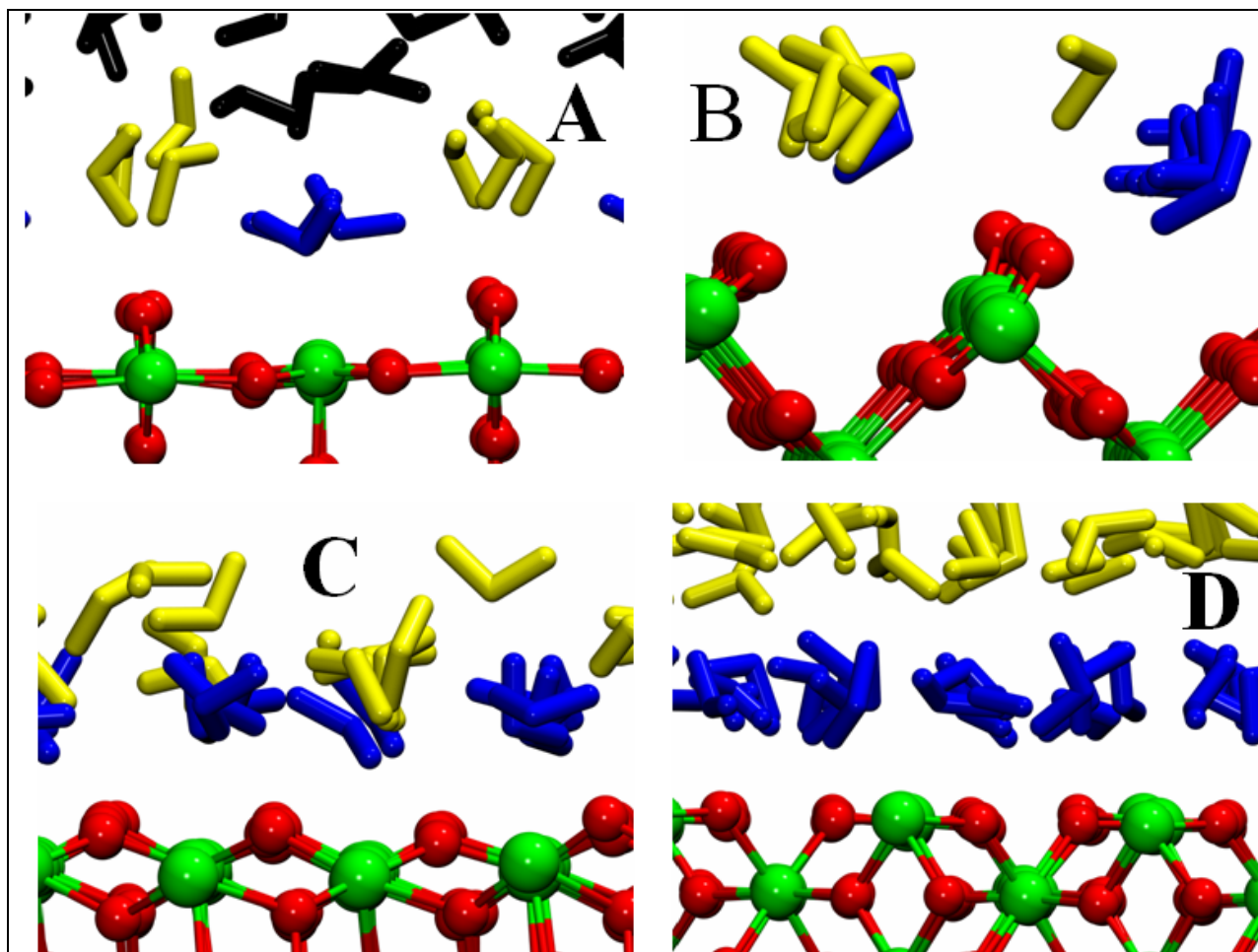


Fig. 1: Representative configurations of various rutile-water interfaces: (A) (110), (B) (100), (C) (101), and (D) (001). (blue- 1 ML, yellow- 2 ML)

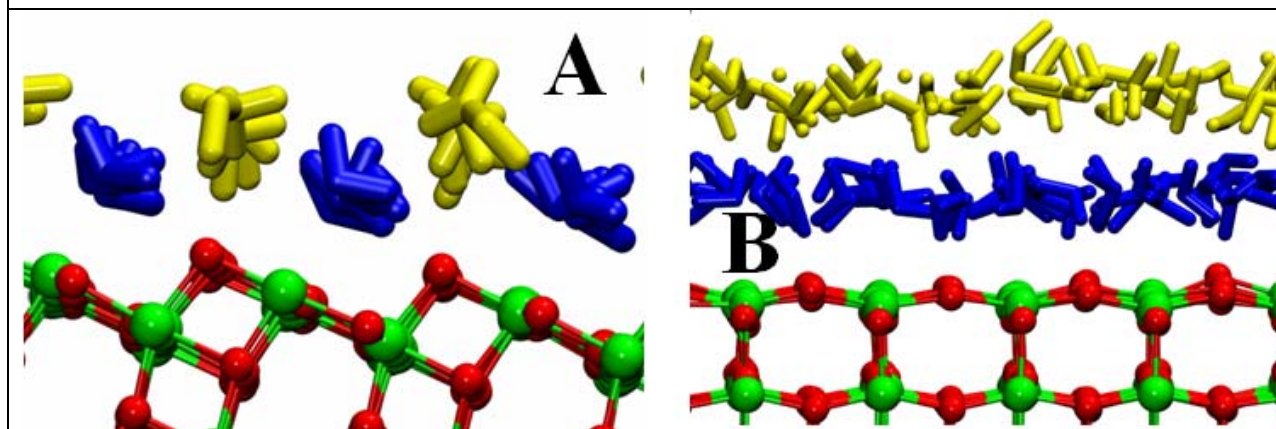


Fig. 2: Representative configurations of various anatase-water interfaces: (A) (101), and (B) (001) (blue- 1 ML, yellow- 2 ML)



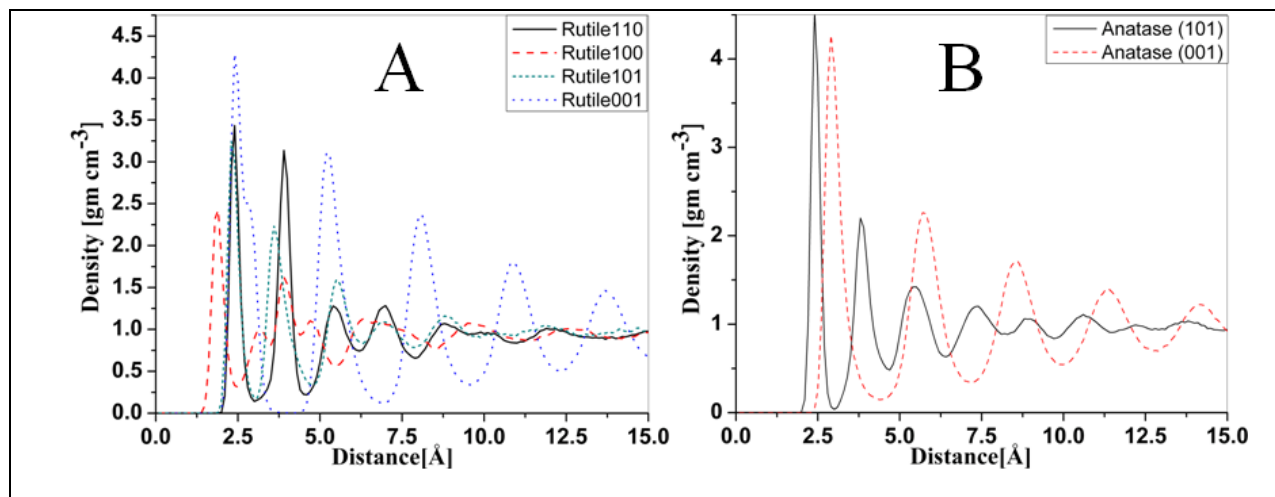


Fig 3: Absolute density ( $\text{gm cm}^{-3}$ ) of water above various planes of (a) rutile and (b) anatase. The plane formed by the first surface titanium atoms was used for projection of the vectors (see text for details).

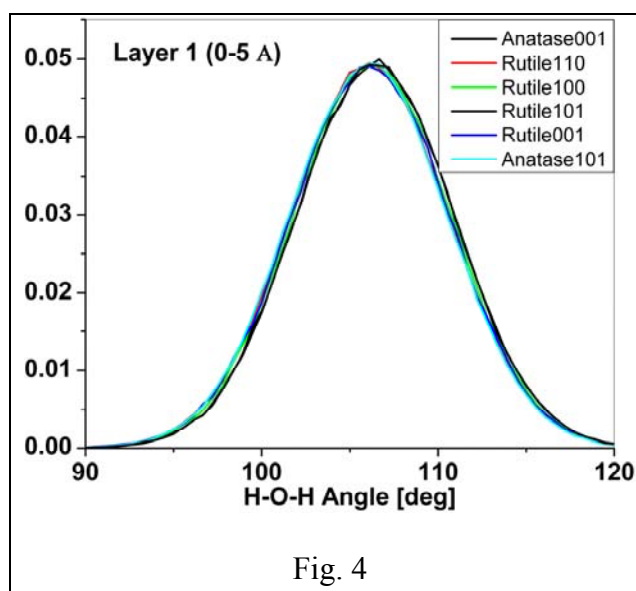


Fig. 4

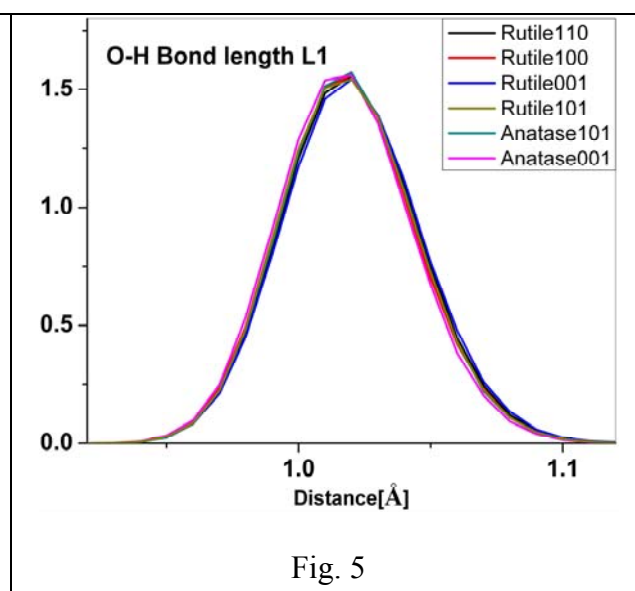


Fig. 5

Fig. 4: Probability distribution of the water H-O-H angle in the adsorbed L1 (0-5  $\text{\AA}$ ) in contact with each surface

Fig. 5: Distribution of the water O-H bond length in the adsorbed monolayer in contact with each surface

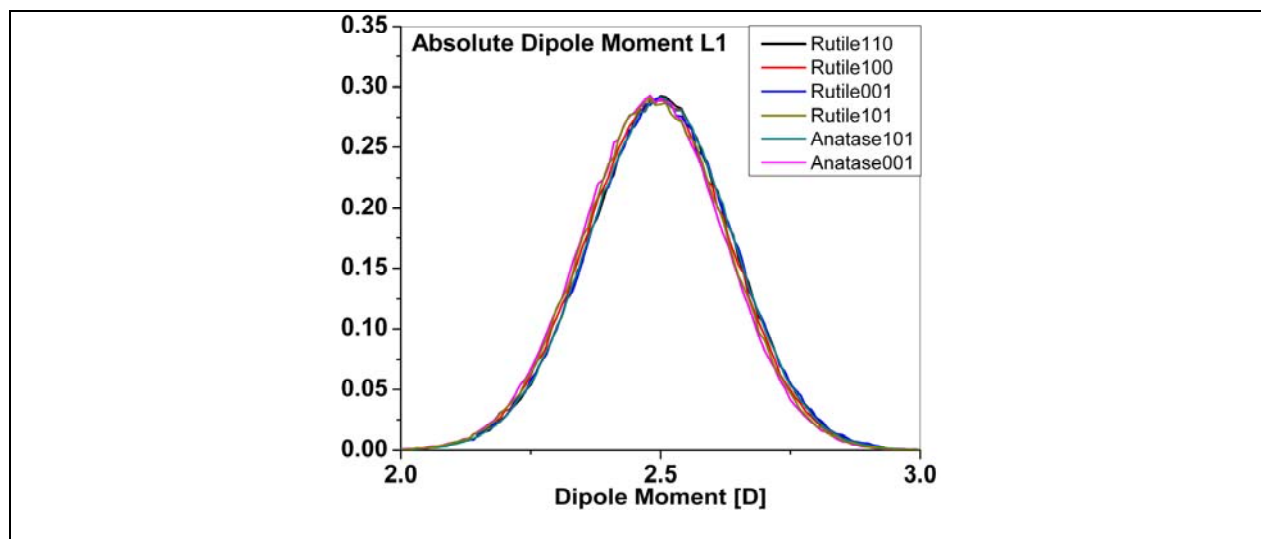


Fig. 6: Distribution of the water absolute dipole moment within 0 to 5 Å from the surface.

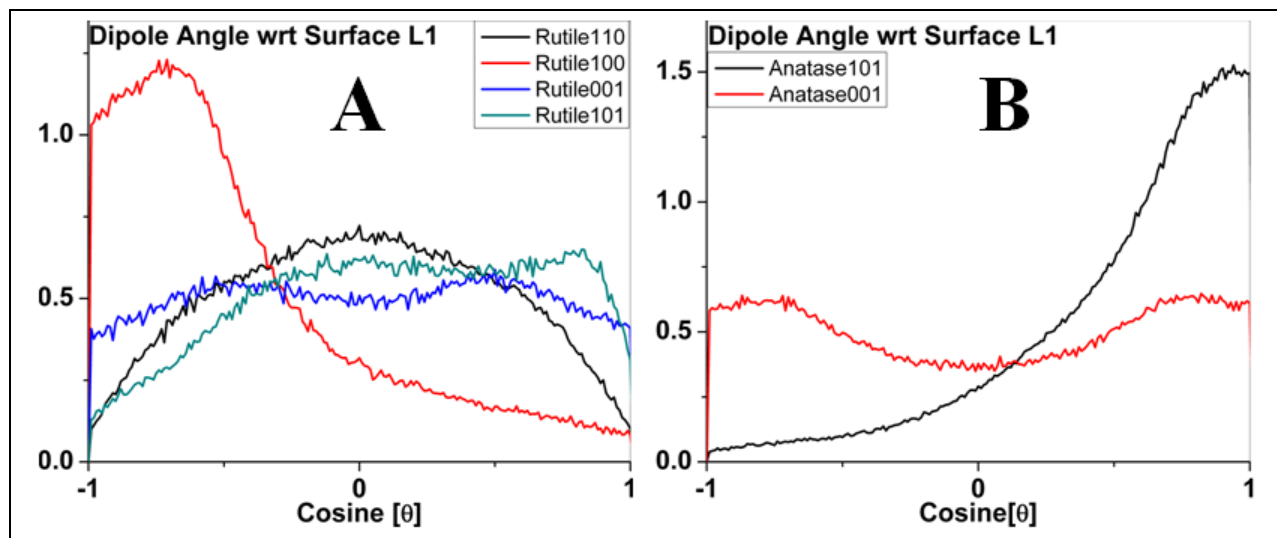


Fig. 7: Distribution of the cosine of angle of water molecules' dipole vectors with respect to the plane of the crystal surfaces,  $\theta$ , within 5 Å from the surface for various faces of (a) rutile, and (b) anatase. A cosine of zero indicates dipole alignment normal to the face, while  $\pm 1$  indicates parallel dipole alignment, oriented parallel, or along, the surface.

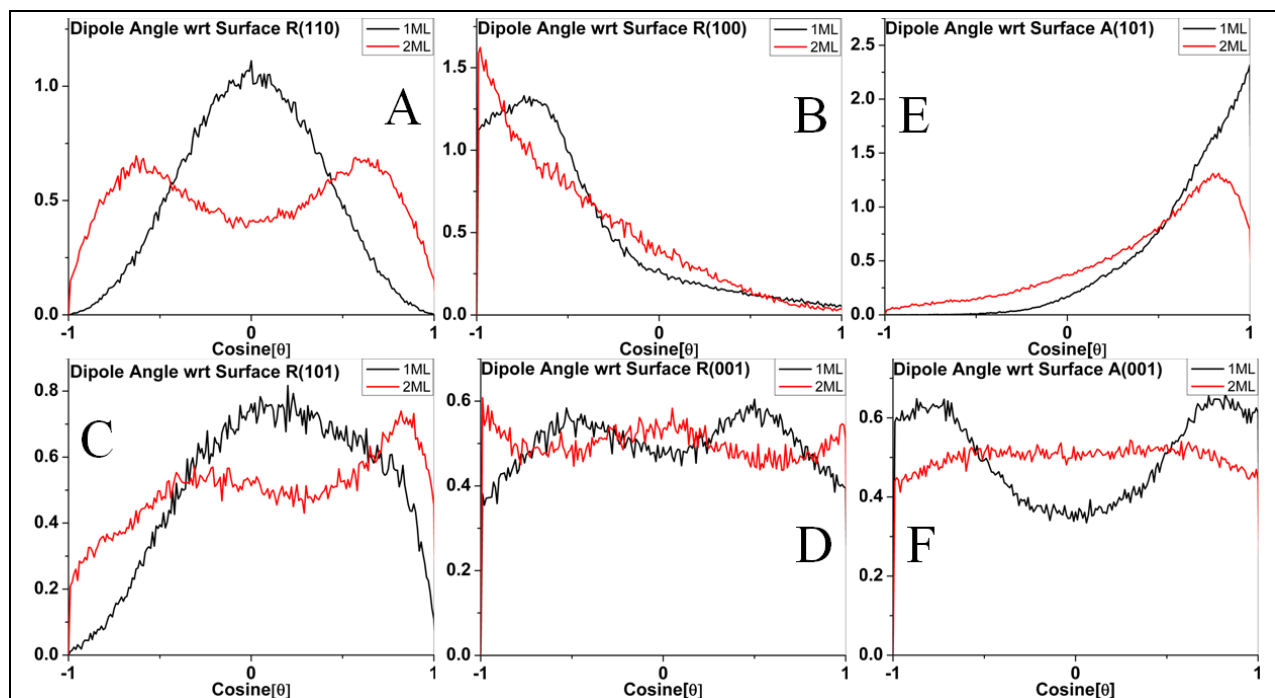


Fig. 8: Distribution of the cosine of angle of the first two layers of water molecules' dipole vectors with respect to the plane of the crystal surfaces,  $\theta$ , for various faces: (A) Rutile (110), (B) Rutile (100), (C) Rutile (101), (D) Rutile (001), (E) Anatase (101), (F) Anatase (001). A cosine of zero indicates dipole alignment normal to the face, while  $\pm 1$  indicates parallel dipole alignment, oriented parallel, or along, the surface.

Phase (surface), X, Y, Z (Å)	System Size
Rutile (110) 26.26, 45.47, 69.490	(TiO <sub>2</sub> ) <sub>630</sub> (H <sub>2</sub> O) <sub>2000</sub>
Rutile(100) 22.97, 26.63, 70.00	(TiO <sub>2</sub> ) <sub>405</sub> (H <sub>2</sub> O) <sub>950</sub>
Rutile(101) 27.33, 27.56, 113.47	(TiO <sub>2</sub> ) <sub>300</sub> (H <sub>2</sub> O) <sub>2468</sub>
Rutile(001) 22.97, 22.97, 124.00	(TiO <sub>2</sub> ) <sub>400</sub> (H <sub>2</sub> O) <sub>1720</sub>
Anatase(101) 71.46, 26.43, 72.680	(TiO <sub>2</sub> ) <sub>1176</sub> (H <sub>2</sub> O) <sub>3162</sub>
Anatase(001) 33.98, 33.98, 124.00	(TiO <sub>2</sub> ) <sub>648</sub> (H <sub>2</sub> O) <sub>3900</sub>

Table I: Details of geometries used

<i>Buckingham potential for TiO<sub>2</sub> and water oxygen : <math>A_{ij} \times \exp(-r_{ij}/\rho_{ij}) - C_{ij}/r_{ij}^6</math></i>			
i – j	$A_{ij}(\text{kcal mol}^{-1})$	$\rho_{ij}(\text{\AA})$	$C_{ij}(\text{kcal mol}^{-1} \text{\AA}^6)$
Ti – O	391049.1	0.194	290.331
Ti – Ti	717647.4	0.154	121.067
O – O	271716.3	0.234	696.888
Ti – O <sub>w</sub>	28593.0	0.265	148.000
<i>Lennard-Jones potential for water: <math>(q_i q_j / r_{ij}) + \epsilon_{ij} [(\sigma_{ij}/r_{ij})^{12} - (\sigma_{ij}/r_{ij})^6]</math></i>			
i – j	$\epsilon_{ij} (\text{kcal mol}^{-1})$	$\sigma_{ij}(\text{\AA})$	
O <sub>w</sub> – O <sub>w</sub>	0.15539	3.5532	
<i>Morse bond potential for water: <math>A_{ij}[1 - \exp(-k_{ij}(r_{ij} - r_{ij}^0))]^2 - A_{ij}</math></i>			
i – j	$A_{ij} (\text{kcal mol}^{-1})$	$k_{ij} (\text{\AA}^{-1})$	$r_{ij}^0 (\text{\AA})$
O <sub>w</sub> – H <sub>w</sub>	101.905	2.347	1.00
<i>Harmonic angle bending potential for water: <math>k/2 \times (\theta - \theta_0)</math></i>			
i – j – k	$\theta_0 \text{ deg}$	$k (\text{kcal mol}^{-1} \text{rad}^{-2})$	
H – O – H	109.47	103.045	
Atomic charges: $q(\text{Ti}) = 2.196 e$ , $q(\text{O}) = -1.098 e$ , $q(\text{O}_w) = -0.82 e$ , $q(\text{H}_w) = 0.41 e$ ; O <sub>w</sub> , H <sub>w</sub> = water oxygen and hydrogen atoms			
Table II: Force field parameters			